Increase in the Iron Content of the Substantia Nigra and Red Nucleus in Multiple Sclerosis/Clinically Isolated Syndrome using 7T MRI

Anna I. Blazejewska[1], Ali Al-Radaideh[2], Samuel Wharton[2], Su Yin Lim[3], Cris S. Constantinescu[3], Richard W. Bowtell[2], and Penny A. Gowland[2]

[1]Sir Peter Mansfield Magnetic Resonance Centre, University of Nottingham, Nottingham, Nottinghamshire, United Kingdom, [2]Sir Peter Mansfield Magnetic Resonance Centre, University of Nottingham, [3]Department of Neurology, Clinical Sciences, University of Nottingham

Introduction Iron deposition in deep grey matter (dGM) structures in multiple sclerosis (MS) has been measured in several studies using T2- and T2*-weighted images [1, 2] and susceptibility weighted images (SWI) [3]. Significant changes associated with increased iron content in MS have been consistently reported for most dGM structures, but the results for the Substantia Nigra (SN) and Red Nucleus (RN) remain inconsistent. Here, we investigate iron deposition in patients with Relapsing-Remitting MS (RRMS) and in patients with CIS (a condition suggestive of early MS). 7T MRI was used to give increased sensitivity to susceptibility effects [4]. Susceptibility mapping was used to overcome the spatial distortions that can affect phase and SWI data [5]. T2*-weighted signals were also used to investigate the effects of spatial changes in the iron distribution. Ventral (SNv) and dorsal (SNd) parts of the SN were considered separately based on reported changes in iron distribution in other neurogenerative diseases [6]. Aim: to assess iron content in the SN and RN of patients with CIS and RRMS compared to healthy controls (HC) using susceptibility mapping and T2*-weighted (T2*w) signals measured at 7T.
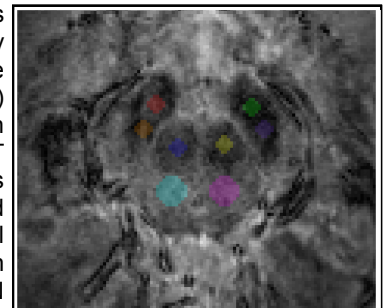

Fig. 1: T2*-weighted image showing ROIs placed in the SNv (red and green), SNd (orange and purple) and RN (blue and yellow). The two ROIs in cyan and magenta are WM regions used for normalisation.
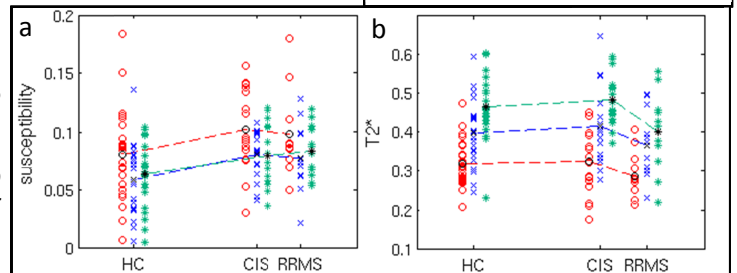
Methods MR images were acquired on a 7T Philips Achieva scanner using a T2*-weighted GRE sequence (TR/TE=150/20ms, flip angle 14, 0.5x0.5x0.5mm, FOV=192x164x25, SENSE=2, scan time=8.5 min) for 12 patients with Relapsing-Remitting (RRMS; age=44.5±10y) and 16 patients with Clinically Isolated Syndrome (CIS; age=37.3±8.5y), and 23 age-matched healthy controls (HC; age=36.7±8.8y). Susceptibility maps were generated from phase data using a k-space threshold method [5]. For each subject, circular ROIs of diameter 3mm were drawn separately on left and right RN and SN in the ventral (SNv) and dorsal (SNd) parts, in 5 slices of the T2*w magnitude images where both structures were most visible (Fig. 1). All of the SN ROIs were positioned to avoid touching ventral and medial boundaries of the structure. Two further ROIs of diameter 5mm were placed on the white matter (WM) in the same slices and used to measure reference values. Mean intensities were calculated on T2*w modulus images and susceptibility maps for SNv, SNd and RN by combining left and right data and normalising using the mean intensity of the WM regions (difference for susceptibility, ratio for T2*w). Normality was checked using the Kolmogorov-Smirnov test. One-way ANOVA testing was performed to test differences between the MS patients and HC for each structure. Scatter plots of susceptibility and 1/T2*w signal were overlaid with the line of best fit for the control data and an ellipse indicating the HC distribution (+/- 1.5s.d.).

Fig. 2: Mean susceptibility (a) and T2* (b) in ○ SNv × SNd and ✳ RN for HC and MS patients (CIS and RRMS).

Results A significant increase in susceptibility was found in combined MS patients versus HC for SNd (p=0.009) and RN (p=0.023) with a trend for SNv (p=0.058). The SN differences were larger for CIS than RRMS, but the difference between CIS and RRMS was not significant (Fig. 2a). The decrease of T2*w signal between HC and MS was not significant (Fig. 2b) although considering the patient groups separately there was a trend for RRMS to have lower T2*w signal than HC and this was significant for the RN (p=0.05). The product of susceptibility and T2*w signals (similar to SWI) did not increase the separation of groups but scatter
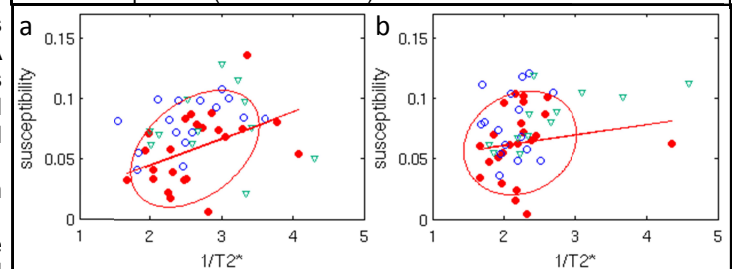

Fig. 3: Scatterplots of susceptibility versus 1/T2*w in (a) SNd and (b) RN. Ellipse indicate population of the ● HC centred at the mean value, outlined by the 1.5 of the standard deviation and oriented parallel to the best fit slope; patients populations were marked by ○ CIS and ▽ RRMS.

plots of susceptibility and 1/T2*w signal (Fig. 3) showed that 10/23 HC, 2/16 CIS and 2/12 RRMS lay below the HC line of best fit. There was no significant variation of susceptibility or T2*w signal with age for HC, or with EDSS for CIS and RRMS patients combined. No differences between the left and right sides were significant.

Discussion Changes consistent with an increase in iron in the SN and RN were found in CIS and RRMS patients using susceptibility mapping at 7T. The lack of variation in iron content over this age range agrees with previous histological measurements [7]; previous studies also found no correlation between iron and EDSS for MS patients [4, 8]. Greater differences in SNd compared to SNv suggest a similar pattern of the iron accumulation in SN to that previously found in Parkinson's disease [6]. Variation across the SN may explain the lack of consistency in previous results; high resolution imaging at 7T allowed specific ROIs to be defined within the SN. The effects of iron accumulation on susceptibility maps and T2*w images are different: susceptibility maps correspond to mean iron concentration, whereas T2*w signals depend on the microscopic iron distribution. There was a trend for susceptibility to change earlier in disease (CIS) than T2*w (RRMS), suggesting that iron accumulation is initially uniform but becomes more heterogeneous later. Future work will include R2* measurements and will investigate how the results relate to whether CIS patients convert to MS.

References [1] Bakshi et al., Arch. Neurol., 2002, 59:62-68; [2] Khalil et al., Multiple Sclerosis, 2009, 15: 1048-1054; [3] Zivadinov et al., Neuroimage, 2012, 59:331-339; [4] Zhang et al., Multiple Sclerosis, 2007, 13:880-883; [5] Wharton et al., MRM, 2010, 63:1292-1304; [6] Fearnley & Lees, Brain, 1991, 114:2283-2301; [7] Halgeren & Sourander, J. Neurochem, 1958, 3:41-52; [8] Zhang at el., J. Neurological Sciences, 2010, 297:76-81.